

A study of some organic reactions using density functional theory

Jon Baker, Max Muir, and Jan Andzelm

Citation: *The Journal of Chemical Physics* **102**, 2063 (1995); doi: 10.1063/1.468728

View online: <http://dx.doi.org/10.1063/1.468728>

View Table of Contents: <http://scitation.aip.org/content/aip/journal/jcp/102/5?ver=pdfcov>

Published by the [AIP Publishing](#)

Articles you may be interested in

[Density functional theory study of the organic functionalization of hydrogenated silicene](#)

J. Chem. Phys. **138**, 194702 (2013); 10.1063/1.4804545

[Some estimates of the surface tension of curved surfaces using density functional theory](#)

J. Chem. Phys. **124**, 144705 (2006); 10.1063/1.2179425

[A density functional theory study of hydroxyl and the intermediate in the water formation reaction on Pt](#)

J. Chem. Phys. **114**, 513 (2001); 10.1063/1.1328746

[Some reasons not to use spin projected density functional theory](#)

J. Chem. Phys. **105**, 6574 (1996); 10.1063/1.472497

[Study of some hydrogen bonded complexes in polar media using density functional theory and SCRF calculations](#)

AIP Conf. Proc. **330**, 151 (1995); 10.1063/1.47870



A study of some organic reactions using density functional theory

Jon Baker, Max Muir, and Jan Andzelm

Biosym Technologies, Inc., 9685 Scranton Road, San Diego, California 92121

(Received 19 July 1994; accepted 12 September 1994)

Twelve organic reactions (six closed shell and six radical) were studied using semiempirical, traditional *ab initio* and density functional methodologies. Full geometry optimizations of all species, both minima and transition states, were performed, and calculated geometries and barrier heights compared with experimental data. Our results demonstrate that although currently available density functionals tend to underestimate barrier heights, especially for radical reactions—in some cases reactions with low barriers are predicted to be essentially barrier free—they provide a significant improvement over standard methods. The adiabatic connection method recently proposed by Becke [J. Chem. Phys. **98**, 5648 (1993)], in which a portion of the exact Hartree–Fock exchange is mixed in to the density functional, looks very promising. © 1994 American Institute of Physics.

I. INTRODUCTION

Density functional methods^{1–6} are being used more and more in computational quantum chemistry and density functional theory (DFT) is emerging as a potentially extremely important predictive tool. The main reason for the increasing use of DFT is, of course, its computational speed; depending on the precise methodology, DFT calculations range from being 2 or 3 times more costly than standard Hartree–Fock calculations to several times faster with the relative speed advantage becoming even greater as the system size increases. This advantage is even more marked when compared to typical post self-consistent field (SCF) methods for incorporating electron correlation (e.g., MP2, CISD) which scale very poorly with system size. Thus with DFT we have a method which includes electron correlation (it is potentially exact if the exact density functional were known) and yet is, at worst, no more expensive than a traditional Hartree–Fock (HF) calculation for large systems.

There are a few disadvantages, however. We should note that there is, as yet, no systematic way to improve the quality of a particular DFT calculation (unlike the use of configuration interaction (CI) or perturbation theory to systematically improve a given Hartree–Fock wave function). In addition, all currently available DFT codes achieve their speed advantage by introducing a significant numerical component into the calculation, complete with the potential loss of accuracy and introduction of numerical “noise” this could entail; thus DFT calculations are not as “clean” as the more traditional *ab initio* approaches.

As far as the accuracy of the results *vis à vis* experiment, conventional wisdom has it that good quality nonlocal DFT calculations employing, say, Becke’s nonlocal exchange functional⁷ in conjunction with the correlation functionals of Lee, Yang, and Parr⁸ (BLYP) or Perdew⁹ (BP), generally give geometries, frequencies, and heats of reaction as good as, if not better than, those obtained from second-order Møller–Plesset perturbation theory (MP2). There is a large body of work validating this claim^{2–6,10–13} and we ourselves have carried out an extensive series of calculations on over a hundred small molecules and several hundred heats of reaction confirming this.¹⁴

However, much of the chemical validation of DFT methods has been done on fairly small systems—such as the set of 52 small molecules in the G2 data base¹⁵—and attention has been focused primarily on the properties of stable, ground state molecules. Metastable species and transition states, necessary for elucidating reaction mechanisms, have received much less attention.

There have, of course, been DFT studies on chemical reactions and transition states commencing with the work of Fan and Ziegler;¹⁶ two recent examples are the papers by Andzelm *et al.*¹⁷ and Stanton and Merz.¹⁸ The majority of such studies to date have been on closed shell systems and the conclusion is again that nonlocal DFT calculations reproduce barrier heights to the same level of accuracy as post SCF calculations in most cases.¹⁸ However, there does appear to be a general trend for barriers to *perhaps* be too low and there are reports circulating that this could be a major problem for radical reactions in particular.¹⁹

There is also evidence that relative energies for larger systems may not be reproduced well in certain cases with the currently available energy functionals; for example, Raghavachari *et al.*²⁰ find dramatic differences in the relative energies of various isomers of C₂₀ calculated using MP2 and BLYP (although the authors seem to suggest that the BLYP results may be the more reliable in this case) and Pople has also reported similar findings for other systems.²¹

In this article we present a study of the relative energetics and barrier heights for twelve sample organic reactions, six of which are formally closed shell and six radical reactions. We have chosen systems which show a range of barrier heights, from a few to in excess of 50 kcal/mol. Our study attempts to answer two questions: (1) How reliable is DFT in reproducing barrier heights and relative energies compared to experiment? (2) How does it perform compared to other commonly used theoretical methods? With these aims in mind we have carried out semiempirical, SCF, and MP2 calculations as well as DFT calculations with the popular BLYP functional^{7,8} and the adiabatic connection method (ACM), a hybrid HF-DFT functional proposed by Becke.²²

II. COMPUTATIONAL DETAILS

The following reactions are examined in this work. (i) *CLOSED SHELL (singlets)*. (1) The rearrangement of acetaldehyde to vinyl alcohol (as an example of keto-enol tautomerism); (2) the addition of ethylene and butadiene to give cyclohexene (the parent Diels–Alder reaction); the unimolecular decompositions of (3) tetrazine and (4) trifluoromethanol; and an examination of the potential energy surface (PES) of cyclobutene focussing specifically on (5) the ring opening of butadiene and (6) the latter's cis(oid)-trans rotational isomerism. (ii) *RADICAL (all doublets)*. Reactions of molecular hydrogen with (1) the fluorine oxide and (2) the hydroxyl radical; (3) ring opening of the cyclopropyl radical; reactions of the methyl radical with (4) ethylene and (5) formaldehyde; and (6) reaction of the hydrogen atom with acetylene.

Seven sets of calculations—MNDO, AM1, HF/3-21G, HF/6-31G*, MP2/6-31G*, BLYP/6-31G*, and ACM/6-31G*—were carried out on each system with full geometry optimization of all species in each case. The six singlet reactions were studied within the restricted closed shell and the six radical reactions within the unrestricted open shell formalisms. We have not done an extensive basis set study, instead selecting 6-31G* as a representative and commonly used basis in calculations of this type. (Note that we used five pure as opposed to six Cartesian components in the *d*-polarization function.) Calculations with the 3-21G basis were done mainly for comparison purposes.

Energies and gradients at the semiempirical, HF and MP2 levels of theory were calculated with GAUSSIAN 90;²³ the BLYP and ACM DFT calculations were done with our DFT-modified version of TURBOMOLE.²⁴ All geometry optimizations, for both transition states and minima, were carried out with the EF algorithm²⁵ using the general purpose stand-alone optimization package OPTIMIZE.²⁶ From a practical point of view, final geometries and Hessians from the SCF calculations were used as input to the higher level MP2 and DFT optimizations; this considerably reduced the CPU time required for the latter calculations, especially for transition states. We used standard convergence criteria of 0.0003 a.u. on the maximum gradient component and either an energy change from the previous cycle of less than 10^{-6} hartree or a maximum predicted displacement of less than 0.0003 a.u. per coordinate.

A few comments are in order as to our DFT methodology. The approach we have used is formally analogous to a standard Hartree–Fock in which the one-electron and two-electron Coulomb terms are exactly the same as in a normal HF calculation, but the exchange terms have been replaced by an exchange–correlation density functional.⁵ Full details will be given elsewhere,²⁷ but suffice it to say that we use an adaptive grid with around 2700–3000 points per hydrogen atom and 4000+ points for first row atoms depending on their particular molecular environments. DFT gradients are calculated *in full* including both functional and weight derivatives and show exact translational invariance. We have also adopted a “standard orientation” similar to that proposed by Gill *et al.*²⁸ which ensures that our DFT energies are “rotationally invariant,” although we do not yet have full

rotational invariance in our gradients.²⁹ Apart from this—the effect of which should be minor—we are fully confident as to the accuracy and stability of our DFT code, for both energies and gradients.

Finally a brief comment on the adiabatic connection method. In Ref. 22 Becke argues that some proportion of the *exact* (HF) exchange energy must be included in any reliable density functional if quantitative accuracy is desired, and proposes a hybrid exchange–correlation functional which is, in essence, a linear combination of several commonly used functionals and a term representing the exact exchange. The coefficients multiplying the various terms were determined by a least-squares fit to results in the G2 data base. In this work we have used essentially the same functionals and coefficients as suggested by Becke [see Eq. (2) in Ref. 22)]. Note that our formalism—which involves calculating all the two-electron integrals for the Coulomb part—enables us to calculate the exchange term *exactly*.

III. RESULTS

A table of total energies calculated for all species examined in this work at all levels of theory is provided in the Appendix. In this section we discuss each reaction in turn, comparing reaction energetics, barrier heights and geometries between each level of theory and with experiment. Relative energies are reported in kcal/mol and we have adopted the standard practice of correcting *all* our *ab initio* energies with the zero point vibrational energy calculated at the Hartree–Fock level, scaled by a factor of 0.89. Hartree–Fock zero-point vibrational energies (ZPVE's) are given in the Table in the Appendix. Unless stated otherwise, experimental geometries were taken from the table of bond lengths and angles in Ref. 30. Schematic diagrams of several of the molecules examined in this study are given in Fig. 1.

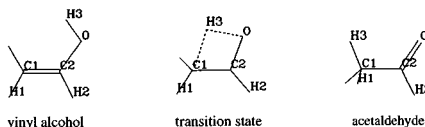
Scheme 1. Vinyl Alcohol→Acetaldehyde

Despite the importance of this tautomerism reaction there is some controversy as to its activation energy in the gas phase; a recent theoretical study by Radom and co-workers argues convincingly that the available experimental data may be suspect.³¹ Consequently, the “experimental” barrier reported in Table I(b) is in fact the G2¹⁵ result from Ref. 31. The heat of reaction, on the other hand, seems fairly well established.³²

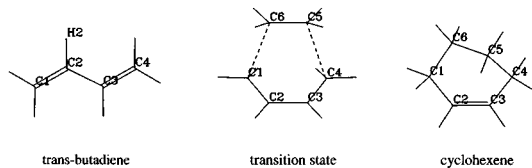
Looking at Scheme 1 we see that there is no clear winner amongst the various theoretical methods. The geometries [Table I(a)] are pretty similar except for the twist angle (dH–CCO) in the transition state which is significantly different between the semiempirical ($\sim 130^\circ$) and *ab initio* ($\sim 150^\circ$) methods. MP2 definitely gives the best agreement with experiment for the geometry of vinyl alcohol, but not so for acetaldehyde. The heat of reaction [Table I(b)] is best predicted by the lower levels of theory (AM1, 3-21G) but the barrier is much too high; better—but still somewhat too high—barrier heights are obtained from the correlated methods (MP2, DFT), but now the heat of reaction is too negative. Overall the energetics are better for DFT than MP2.

There are some trends that are apparent when comparing the geometrical parameters that are fairly general for all the

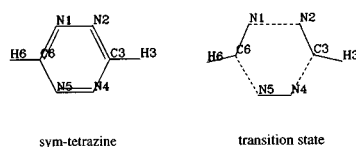
Scheme 1



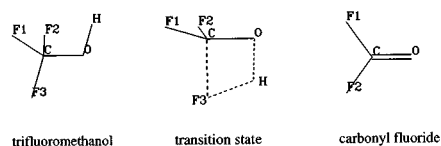
Scheme 2



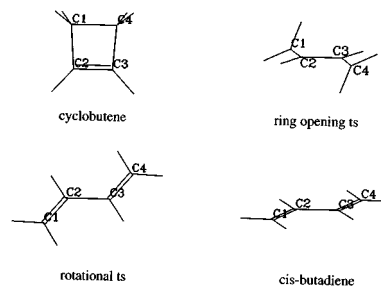
Scheme 3



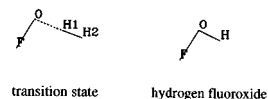
Scheme 4



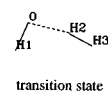
Scheme 5



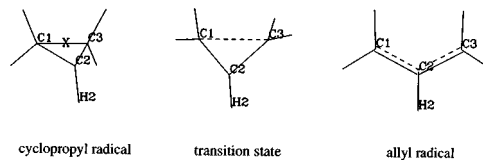
Scheme 6



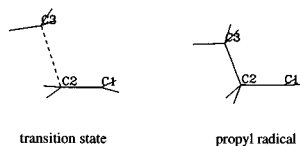
Scheme 7



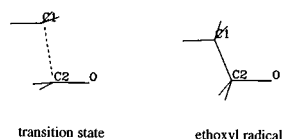
Scheme 8



Scheme 9



Scheme 10



Scheme 11

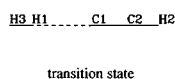


FIG. 1. Schematic diagrams of reactants, products and transition states for the twelve organic reactions investigated. Selected geometrical parameters and reaction energetics are shown in Tables I–XI.

species studied in this work. The first—which is well known—is that standard bond lengths are usually longer at the MP2 level than they are at HF. The second is that bond lengths usually further increase between MP2 and BLYP but

decrease from BLYP to ACM, often to below the MP2 values. This decrease is a consequence of the presence in the ACM functional of a proportion of the true HF exchange.

Looking at the correlated methods (MP2, BLYP, ACM)

TABLE I. Vinyl alcohol→acetaldehyde. (a) Selected geometrical parameters. (b) Energies (relative to vinyl alcohol; kcal/mol).

Param.	MNDO	AM1	3-21G	HF	MP2	BLYP	ACM	Expt.
(a)								
Vinyl Alcohol (C_s) ^a								
r_{C_2-O}	1.357	1.372	1.377	1.347	1.368	1.377	1.357	1.369
$r_{C_1-C_2}$	1.350	1.336	1.314	1.318	1.337	1.345	1.334	1.335
r_{O-H_3}	0.948	0.968	0.966	0.949	0.975	0.983	0.969	0.962
$r_{C_2-H_2}$	1.099	1.103	1.069	1.073	1.085	1.094	1.087	1.080
$a_{C_1C_2O}$	126.5	125.1	127.1	127.0	126.8	127.4	127.4	126.0
$a_{C_2OH_3}$	113.4	109.0	112.7	110.3	108.1	108.0	108.6	108.5
Transition State (C_1)								
r_{C_2-O}	1.280	1.296	1.282	1.252	1.295	1.302	1.283	
$r_{C_1-C_2}$	1.458	1.424	1.421	1.421	1.406	1.419	1.409	
$r_{C_2-H_2}$	1.090	1.096	1.072	1.081	1.092	1.102	1.094	
$r_{C_1-H_3}$	1.546	1.572	1.550	1.519	1.520	1.542	1.509	
r_{O-H_3}	1.267	1.335	1.272	1.234	1.294	1.315	1.284	
$a_{C_1C_2O}$	103.6	107.0	108.3	109.2	110.9	111.2	110.6	
$a_{OH_3C_1}$	99.5	97.3	101.5	104.3	104.3	103.5	104.6	
$d_{H_1C_1C_2O}$	-130.0	-137.5	-150.4	-152.4	-153.4	-154.1	-154.1	
Acetaldehyde (C_s)								
r_{C_2-O}	1.221	1.231	1.208	1.188	1.221	1.223	1.209	1.210
$r_{C_1-C_2}$	1.517	1.490	1.507	1.504	1.517	1.520	1.504	1.515
$r_{C_2-H_2}$	1.112	1.114	1.087	1.095	1.112	1.125	1.114	1.128
$a_{C_1C_2O}$	125.0	123.5	124.8	124.4	125.0	124.9	124.8	124.1
(b)								
EA	91.2	73.6	76.9	70.0	55.4	48.7	52.3	39.4
ΔH_f	-7.4	-8.0	-9.1	-17.8	-17.5	-16.1	-15.5	-9.8

^aExperimental geometry for vinyl alcohol taken from Ref. 31.

the energetics are not particularly impressive, with errors of around 10 kcal/mol in the barrier height and 6 kcal/mol in the heat of reaction. This reaction appears to require large basis sets and extensive electron correlation in order to obtain energetic data that compares well with experimental values.³³

Scheme 2. Butadiene+Ethylene→Cyclohexene

The *parent* Diels–Alder reaction has been the subject of a great many theoretical studies.³⁴ Despite claims of diradical intermediates,³⁵ it now seems well established that this is a synchronous and concerted reaction.^{34,36} (A similar conclusion has also been reached on the related Cope rearrangement.³⁷)

Apart from a few minor differences—for example, the C–C single bond lengths in cyclohexene are noticeably shorter with AM1—the various theoretical methods all give a similar picture as to the geometries of all species involved in this reaction; in particular, the transition state geometry is remarkably similar with a $C\cdots C$ forming bond length of around 2.2 Å in all cases. The energetics are also similar, although there is a fair spread of values, especially for the barrier height. The best predictions for the barrier are from

AM1, BLYP, and ACM, respectively, in that order. Surprisingly, we were unable to find an experimental value for the heat of reaction (Table II).

Scheme 3. Tetrazine→2HCN+N₂

This is an interesting reaction (see Table III), not least for the possibility of a single-step triple dissociation; this has been investigated theoretically by Scheiner *et al.*³⁹ who concluded that the triple dissociation was in fact highly plausible. As far as the geometries go, the best predictions are clearly those from the ACM method, especially for tetrazine itself and also for nitrogen. For the transition states, all the *ab initio* methods have similar geometrical parameters, but there are marked differences between these and the semiempirical parameters, with the dissociating $N\cdots N$ bonds being noticeably shorter and the dissociating $C\cdots N$ bonds longer, particularly for AM1; the NCN and NCH angles are also around 10° smaller and 20° larger, respectively.

Energetically, the semiempirical methods show very poor results, with the calculated barrier being far too high and the heat of reaction significantly in error (by over 50 kcal/mol for MNDO which erroneously predicts the reaction to be *endothermic*). The HF calculations aren't much better, but the correlated results are at least qualitatively correct

TABLE II. Butadiene+ethylene→cyclohexene. (a) Selected geometrical parameters. (b) Energies (relative to reactants; kcal/mol).

Param.	MNDO	AM1	3-21G	HF	MP2	BLYP	ACM	Expt.
(a)								
trans-Butadiene (C_{2h})								
rC_1-C_2	1.344	1.335	1.320	1.323	1.342	1.353	1.340	1.349
rC_2-C_3	1.465	1.451	1.467	1.468	1.456	1.462	1.455	1.467
$aC_1C_2H_2$	118.6	120.7	119.9	119.6	119.6	119.3	119.4	120.9
$aC_1C_2C_3$	125.7	123.4	124.0	124.1	123.7	124.5	124.3	124.4
Ethylene (D_{2h})								
$rC=C$	1.335	1.326	1.315	1.317	1.335	1.341	1.330	1.339
$rC-H$	1.089	1.098	1.074	1.076	1.085	1.095	1.088	1.087
$aCCH$	123.2	122.7	121.9	121.8	121.7	121.9	121.8	121.3
Transition state (C_s)								
rC_2-C_3	1.416	1.397	1.394	1.393	1.412	1.416	1.410	
rC_1-C_2	1.387	1.382	1.370	1.377	1.380	1.395	1.377	
rC_1-C_6	2.167	2.119	2.210	2.202	2.286	2.294	2.301	
rC_5-C_6	1.390	1.382	1.376	1.383	1.382	1.398	1.378	
$aC_1C_2C_3$	123.4	121.2	121.5	121.5	121.8	122.2	122.1	
$aC_3C_4C_5$	100.6	99.3	101.6	102.6	101.6	102.4	101.7	
$aC_4C_5C_6$	111.0	109.9	109.1	109.2	109.0	109.2	109.0	
Cyclohexene (C_2)								
rC_2-C_3	1.346	1.337	1.318	1.321	1.342	1.348	1.337	1.334
rC_1-C_2	1.504	1.483	1.515	1.509	1.504	1.520	1.505	1.50
rC_1-C_6	1.541	1.517	1.541	1.531	1.528	1.550	1.532	1.52
rC_5-C_6	1.539	1.514	1.540	1.529	1.526	1.547	1.529	1.54
$aC_1C_2C_3$	123.8	123.3	123.7	123.7	123.3	123.5	123.5	123.4
$aC_3C_4C_5$	114.0	112.5	111.5	111.8	111.5	112.1	112.0	112.0
$aC_4C_5C_6$	114.2	111.4	110.0	110.8	110.4	111.0	110.9	110.9
(b)								
EA	49.7	23.7	36.7	46.2	32.3	21.3	20.3	25 ^a
ΔH_f	-34.2	-36.1	-39.5	-38.6	-35.5	-32.5	-47.1	

^aFrom Ref. 36.

with the ACM energetics being clearly the best. Both of the DFT methods are overall better than MP2; the latter method predicts a heat of reaction that is far too negative.

Scheme 4. $CF_3OH \rightarrow CF_2O + HF$

This reaction (see Table IV), which is thought to be of some importance in atmospheric chemistry as the main decomposition pathway for trifluoromethanol, has recently been studied at a fairly high level of theory by Francisco,⁴² who predicts a barrier height of 45.1 ± 2 kcal/mol. In the absence of experimental data, we have taken this as our “experimental” value in Table IV(b). The heat of reaction has been estimated from heats of formation of the separate species as quoted also from ref. 42.

We were unable to find an experimental geometry for trifluoromethanol, but for carbonyl fluoride and hydrogen fluoride the HF/6-31G* values clearly show the best agreement with experiment, although the FCF angle in the former is too low. Of the correlated methods, ACM is the best in this

regard. Note that both the C–F and C–O bond lengths in trifluoromethanol are predicted to be significantly shorter at HF/6-31G* than with the other theoretical methods; note also the far too short bond length in HF at the AM1 level. The predicted *ab initio* transition state geometries are very similar but are noticeably different from the two semiempirical methods, which predict much shorter dissociating C···F bond lengths and longer C–O and O···H bonds.

None of the methods give a particularly good picture of the energetics. MP2 is best overall, showing excellent agreement with Francisco’s theoretical barrier height,⁴² although the heat of reaction is too endothermic; the next best is probably ACM. The closest agreement with the experimental heat of reaction is with AM1 which, however, gives much too high a barrier. The barrier with MNDO is even worse, being twice the predicted value. As was the case with vinyl alcohol/acetaldehyde, this reaction requires larger basis sets than 6-31G* for an adequate treatment of the energetics, particularly for CF_2O .⁴²

TABLE III. Tetrazine \rightarrow 2HCN+N₂. (a) Selected geometrical parameters. (b) Energies (relative to tetrazine; kcal/mol).

Param.	MNDO	AM1	3-21G	HF	MP2	BLYP	ACM	Expt.
(a)								
Tetrazine (D_{2h}) ^a								
rN_1-N_2	1.273	1.278	1.331	1.290	1.340	1.347	1.320	1.321
rN_1-C_6	1.371	1.383	1.329	1.318	1.345	1.353	1.337	1.334
rC_3-H_3	1.094	1.106	1.064	1.071	1.086	1.094	1.086	
$aN_1C_6H_6$	121.7	123.6	124.7	125.1	127.1	127.2	126.5	127.4
Transition state (C_{2v})								
rN_4-N_5	1.130	1.134	1.156	1.139	1.200	1.189	1.164	
rN_1-N_2	1.717	1.495	1.850	1.868	1.844	1.948	1.948	
rC_3-N_2	1.202	1.220	1.196	1.187	1.234	1.227	1.208	
rC_3-N_4	1.864	1.956	1.762	1.769	1.679	1.747	1.765	
rC_3-H_3	1.069	1.079	1.060	1.066	1.081	1.088	1.079	
$aN_2C_3N_4$	113.2	115.7	124.7	125.1	127.1	125.9	125.0	
$aN_1C_6H_6$	151.7	149.7	133.3	132.5	126.8	129.9	132.3	
Hydrogen cyanide								
$rC-N$	1.160	1.160	1.137	1.133	1.176	1.169	1.157	1.135
$rC-H$	1.055	1.069	1.050	1.059	1.069	1.077	1.071	1.066
Nitrogen								
$rN-N$	1.104	1.106	1.083	1.078	1.131	1.118	1.104	1.098
(b)								
EA	97.5	72.6	44.7	71.3	40.5	29.9	47.8	51.8 ^b
ΔH_f	11.3	-24.3	-83.1	-71.2	-72.4	-39.6	-28.7	-46.4 ^c

^aExperimental geometry for tetrazine taken from Ref. 38.^bFrom Ref. 39.^cCalculated from heats of formation in Ref. 40.TABLE IV. CF₃OH \rightarrow CF₂O+HF. (a) Selected geometrical parameters. (b) Energies (relative to trifluoromethanol; kcal/mol).

Param.	MNDO	AM1	3-21G	HF	MP2	BLYP	ACM	Expt.
(a)								
Trifluoromethanol (C_s)								
$rC-O$	1.391	1.387	1.343	1.331	1.351	1.367	1.348	
$rC-F_3$	1.344	1.352	1.327	1.305	1.332	1.347	1.326	
$rO-H$	0.949	0.968	0.966	0.950	0.974	0.982	0.969	
$aOCF_3$	108.1	106.9	108.9	108.8	108.3	108.1	108.4	
$aCOH$	114.9	109.2	114.8	110.3	108.3	107.9	108.6	
Transition State (C_s)								
$rH-F_3$	1.170	1.221	1.178	1.185	1.193	1.227	1.188	
$rC-O$	1.324	1.325	1.262	1.241	1.263	1.274	1.258	
$rC-F_3$	1.500	1.469	1.708	1.740	1.720	1.778	1.741	
$rO-H$	1.439	1.447	1.268	1.204	1.256	1.240	1.239	
$aOCF_3$	90.8	93.1	88.3	88.6	91.0	89.8	90.0	
$aCOH$	83.0	82.7	84.6	83.0	80.8	82.1	81.3	
Carbonyl Fluoride (C_{2v}) ^a								
$rC-O$	1.219	1.220	1.157	1.169	1.188	1.193	1.179	1.17
$rC-F_1$	1.316	1.328	1.291	1.322	1.328	1.342	1.318	1.32
aF_1CF_2	111.8	111.0	108.3	108.4	107.5	107.6	107.8	112.5
Hydrogen Fluoride								
$rH-F$	0.956	0.826	0.937	0.912	0.935	0.946	0.932	0.917
(b)								
EA	91.2	66.0	57.9	59.5	43.9	34.0	41.0	45.1 ^b
ΔH_f	16.7	6.4	30.0	15.9	11.9	12.5	15.8	5.6 ^b

^aExperimental geometry for carbonyl fluoride taken from Ref. 41.^bFrom Ref. 42.

TABLE V. Cyclobutene→*trans*-butadiene→*cis*-butadiene. (a) Selected geometrical parameters. (b) Energies (ring opening) (relative to cyclobutene; kcal/mol). (c) Energies (rotation) (relative to *cis*-butadiene; kcal/mol).

Param.	MNDO	AM1	3-21G	HF	MP2	BLYP	ACM	Expt.
(a)								
Cyclobutene (C_{2v})								
rC_2-C_3	1.355	1.354	1.326	1.323	1.347	1.352	1.340	1.342
rC_1-C_2	1.524	1.522	1.539	1.515	1.513	1.529	1.513	1.517
rC_1-C_4	1.568	1.566	1.593	1.562	1.564	1.586	1.565	1.566
$aC_1C_4C_3$	86.0	86.0	85.0	85.5	85.9	85.6	85.7	85.8
$aC_2C_3C_4$	94.0	94.0	95.0	94.5	94.1	94.4	94.3	94.2
Ring-opening transition state (C_2)								
rC_1-C_2	1.402	1.389	1.369	1.369	1.379	1.385	1.379	
rC_2-C_3	1.417	1.428	1.421	1.413	1.423	1.440	1.420	
rC_1-C_4	2.129	2.119	2.138	2.130	2.133	2.161	2.142	
$aC_1C_4C_3$	74.3	74.5	73.4	73.5	73.7	73.6	73.6	
$aC_2C_3C_4$	103.5	103.8	104.3	104.3	104.0	104.5	104.3	
$dC_1C_2C_3C_4$	21.7	18.7	21.8	22.0	22.2	20.0	21.3	
<i>trans</i> -butadiene (C_{2h}) ^a								
Rotational transition state (C_2)								
rC_1-C_2	1.341	1.331	1.316	1.319	1.340	1.345	1.334	
rC_2-C_3	1.472	1.457	1.491	1.490	1.483	1.496	1.484	
$aC_1C_2C_3$	126.0	124.4	123.7	124.5	123.6	124.8	124.6	
$dC_1C_2C_3C_4$	93.3	89.9	102.2	102.1	101.6	100.0	100.7	
<i>cis</i> -butadiene (C_2)								
rC_1-C_2	1.343	1.335	1.319	1.322	1.343	1.322	1.338	
rC_2-C_3	1.467	1.450	1.477	1.477	1.469	1.478	1.467	
$aC_1C_2C_3$	127.4	125.4	124.8	125.3	124.1	125.3	125.5	
$dC_1C_2C_3C_4$	44.3	13.3	38.2	39.0	37.8	38.5	32.5	
(b)								
EA	49.8	35.5	40.0	45.2	35.9	29.8	36.1	32.9 ^b
ΔH_f	-11.4	-2.1	-15.8	-19.0	-13.5	-8.7	-15.0	-8.2 ^b
(c)								
EA	0.2	1.1	2.6	2.7	3.0	4.0	3.5	3.9 ^c
ΔH_f	-0.3	-0.8	-2.7	-3.0	-2.6	-3.8	-3.5	-2.5 ^d

^aFor geometrical parameters see Table II(a).^bFrom Ref. 43.^cFrom Ref. 45.^dFrom Ref. 44.**Scheme 5. Cyclobutene→*trans*-butadiene→*cis*-butadiene**

Both the ring opening and the rotational isomerization in this system have been extensively studied.^{43–45} Ring opening occurs via a C_2 transition state which all theoretical methods predict to be structurally very similar. The rotational transition state also has C_2 symmetry and is again structurally similar at all levels of theory except for the twist (dihedral) angle, which is lower by around 10° with the semiempirical methods. It is now well established theoretically^{46,47} that *cis*-butadiene also has a C_2 structure, i.e., is nonplanar, the planar (C_{2v}) form being a transition state between two equivalent C_2 forms (although the barrier is less than 1 kcal/mol). The twist angle is predicted to be around 38° by all the *ab*

initio methods (except ACM which is some 6° lower), in excellent agreement with previous theoretical estimates.^{46,47}

The MNDO and AM1 values are too high and far too low, respectively, although the other parameters are in good agreement. The geometry of cyclobutene itself is well reproduced at virtually all levels of theory; the ACM parameters are particularly good (Table V).

For the ring opening reaction, the best energetics are clearly with BLYP, the other *ab initio* methods predicting heats of reaction that are too negative. For the rotational isomerism all the *ab initio* methods give similar energetics, generally in very good agreement with experiment. The semiempirical barriers are too low and the heats of reaction too high, respectively, especially for MNDO.

TABLE VI. $\text{FO} + \text{H}_2 \rightarrow \text{FOH} + \text{H}$. (a) Selected geometrical parameters. (b) Energies (relative to reactants; kcal/mol).

Param.	MNDO	AM1	3-21G	HF	MP2	BLYP	ACM	Expt.
(a)								
Fluorine oxide radical								
$r_{\text{F-O}}$	1.225	1.251		1.327	1.344	1.383	1.345	1.358
Hydrogen								
$r_{\text{H-H}}$	0.663	0.677	0.735	0.730	0.738	0.748	0.743	0.741
Transition state (C_s)								
$r_{\text{F-O}}$	1.256	1.334	1.610	1.363	1.371	1.452	1.398	
$r_{\text{O-H}_1}$	1.217	1.178	1.162	1.168	1.241	1.054	1.136	
$r_{\text{H}_1-\text{H}_2}$	0.860	0.835	1.059	0.945	0.876	1.240	0.992	
a_{FOH_1}	111.1	107.0	101.2	100.9	101.8	99.5	101.4	
$a_{\text{OH}_1\text{H}_2}$	177.4	176.0	159.9	177.6	179.3	174.3	178.6	
Hydrogen Fluoroxide (C_s)								
$r_{\text{F-O}}$	1.277	1.367	1.439	1.377	1.446	1.469	1.423	1.442
$r_{\text{O-H}}$	0.964	0.971	0.976	0.952	0.979	0.989	0.975	0.96
r_{FOH}	107.9	103.9	99.0	99.7	97.0	96.8	97.9	97.2
(b)								
EA	41.3	21.0		36.1	22.0	14.7	16.3	17.4 ^a
ΔH_f	12.4	13.1		15.0	-1.5	16.9	12.9	3.9 ^a

^aFrom Ref. 48.**Scheme 6. $\text{FO} + \text{H}_2 \rightarrow \text{FOH} + \text{H}$**

As with trifluoromethanol (Scheme 4) this reaction may play a role in atmospheric chemistry.⁴⁸ Like the former reaction, experimental data on the barrier height is not readily available so we have again taken as our “experimental” bar-

rier the quadratic CI value of Francisco.⁴⁸ The heat of reaction has been estimated from heats of formation of the separate species (Table VI).

There are some significant differences in the predicted geometries between the semiempirical and *ab initio* calcula-

TABLE VII. $\text{OH} + \text{H}_2 \rightarrow \text{H}_2\text{O} + \text{H}$. (a) Selected geometrical parameters. (b) Energies (relative to reactants; kcal/mol).

Param.	MNDO	AM1	3-21G	HF	MP2	BLYP	ACM	Expt.
(a)								
Hydroxyl radical								
$r_{\text{O-H}}$	0.937	0.948	0.986	0.959	0.980	0.995	0.980	
Hydrogen ^a								
Transition state (C_s)								
$r_{\text{O-H}_1}$	0.941	0.953	0.978	0.956	0.980	0.992	0.978	
$r_{\text{O-H}_2}$	1.279	1.271	1.153	1.185	1.293	1.414	1.332	
$r_{\text{H}_2-\text{H}_3}$	0.797	0.776	0.976	0.922	0.841	0.821	0.834	
$a_{\text{H}_1\text{OH}_2}$	106.0	105.0	102.6	100.4	98.8	99.3	99.4	
$a_{\text{OH}_2\text{H}_3}$	175.2	160.7	166.6	170.6	166.3	166.3	166.7	
Water (C_{2v})								
$r_{\text{O-H}}$	0.943	0.961	0.967	0.948	0.969	0.980	0.966	0.958
a_{HOH}	106.8	103.5	107.7	105.6	104.1	103.0	104.0	104.5
(b)								
EA	30.7	11.5	25.5	26.5	12.7	-0.8	3.3	3.95 ^b
ΔH_f	-9.8	-2.6	8.7	2.0	-16.9	-5.2	-7.5	-14.6 ^b

^aFor geometrical parameters see Table VI(a).^bFrom Ref. 48.

TABLE VIII. Cyclopropyl radical→allyl radical. (a) Selected geometrical parameters. (b) Energies (relative to cyclopropyl radical; kcal/mol).

Param.	MNDO	AM1	3-21G	HF	MP2	BLYP	ACM	Expt.
(a)								
Cyclopropyl radical (C_3)								
$r_{C_1-C_2}$	1.478	1.454	1.486	1.470	1.469	1.479	1.467	
$r_{C_2-C_3}$	1.478	1.454	1.486	1.470	1.469	1.479	1.467	
$r_{C_1-C_3}$	1.547	1.519	1.535	1.517	1.527	1.553	1.529	
r_{C_2-H}	1.058	1.064	1.067	1.072	1.081	1.091	1.083	
a_{XC_2H}	180.0	180.0	139.1	138.8	138.8	141.4	141.3	
Transition state (C_1)								
$r_{C_1-C_2}$	1.437	1.433	1.484	1.471	1.469	1.396	1.382	
$r_{C_2-C_3}$	1.443	1.421	1.435	1.416	1.365	1.470	1.464	
$r_{C_1-C_3}$	1.955	1.938	1.980	1.983	1.990	2.035	2.014	
r_{C_2-H}	1.070	1.070	1.071	1.075	1.083	1.093	1.085	
Allyl radical (C_{2v})								
$r_{C_1-C_2}$	1.397	1.383	1.389	1.391	1.378	1.395	1.385	
$r_{C_2-C_3}$	1.397	1.383	1.389	1.391	1.378	1.395	1.385	
$r_{C_1-C_3}$	2.491	2.439	2.455	2.462	2.438	2.480	2.459	
r_{C_2-H}	1.097	1.105	1.076	1.078	1.088	1.098	1.091	
(b)								
EA	23.1	24.5	19.6	24.1	35.5	18.1	24.7	22.0 ^a
ΔH_f	-25.2	-29.0	-43.2	-34.6	-21.7	-32.6	-26.8	-22.8 ^a

^aFrom Ref. 50.

tions. For both FO and H₂ the semiempirical bond lengths are much too short, and for FOH the F–O bond is too short and the FOH angle too large. Overall, the best agreement with experiment is with MP2. (There were problems achieving SCF convergence during the 3-21G optimization of FO, so no F–O bond length or energetics are reported for this theoretical model.) The transition state structure is in reasonable accord for all methods; they all predict—not unexpectedly—increases in both the F–O and H–H bond lengths as the new O–H bond is formed. If the somewhat dubious 3-21G results are ignored, then the BLYP parameters show the most disagreement with the other methods.

None of the theoretical methods gives a particularly good heat of reaction; the best is ACM which also gives very good agreement with Francisco's theoretical barrier height. MP2 erroneously predicts the reaction to be *exothermic*, although the absolute error is actually smaller in magnitude than for the other methods, which are all too endothermic. This result is probably due to spin contamination (of which more later) in the underlying UHF wave function for FO.

Scheme 7. OH+H₂→H₂O+H

This reaction has been the subject of considerable theoretical and experimental study. Francisco⁴⁸ used it to calibrate his study on the related reaction involving FO (Scheme 6), and our reported experimental results are taken from this source (see Table VII).

The changes in the calculated geometrical parameters fail to adequately demonstrate the major differences between

the potential energy surface for this reaction as calculated with BLYP vs the other theoretical methods. The forming O···H bond in the transition state is significantly longer with BLYP than with the other approaches, but this is the only really noticeable difference. The major impact is in the energetics with the BLYP barrier being apparently *negative*, i.e., the energy of the “transition state” is *lower* than that of the reactants! This is not an artefact of, e.g., the quadrature grid, but appears to be a genuine problem with the functional itself. We have carried out a detailed study of the BLYP PES for this system, along with several other functionals; our findings will be published in full elsewhere,⁴⁹ but the explanation for the negative barrier is that, unlike for the other methods, the approach of the OH radical to H₂ is *attractive* and before reaction, i.e., abstraction of H, occurs, the system forms a “metastable complex” which subsequently decomposes to H₂O+H via a transition state which has a *lower* energy than that of OH+H₂; thus the transition state found is that for decomposition of the “metastable complex” and *not* that for the studied reaction.

Inclusion of some of the exact HF exchange to the energy functional, as per the ACM method, rectifies the situation and restores the more typical repulsive potential, complete with genuine transition state. In this particular case, the agreement with the experimental barrier height is excellent. Although ACM gives a good barrier, the heat of reaction is not well predicted; in fact, only MP2 gives a reasonable value here (both the Hartree–Fock calculations erroneously predict the heat of reaction to be endothermic).

TABLE IX. Methyl radical+ethylene→propyl radical. (a) Selected geometrical parameters. (b) Energies (relative to reactants; kcal/mol).

Param.	MNDO	AM1	3-21G	HF	MP2	BLYP	ACM	Expt.
(a)								
Methyl radical (D_{3h})								
r_{C-H}	1.078	1.086	1.072	1.073	1.078	1.090	1.083	1.08
Ethylene (D_{2h}) ^a								
Transition state (C_s)								
$r_{C_2-C_3}$	2.222	2.176	2.269	2.246	2.262	2.427	2.389	
$r_{C_1-C_2}$	1.327	1.358	1.375	1.382	1.344	1.364	1.352	
$a_{C_1C_2C_3}$	104.7	97.6	107.8	109.1	109.5	110.5	110.1	
Propyl radical (C_s)								
$r_{C_2-C_3}$	1.533	1.513	1.552	1.537	1.537	1.563	1.542	
$r_{C_1-C_2}$	1.484	1.463	1.508	1.501	1.491	1.499	1.489	
$a_{C_1C_2C_3}$	114.0	111.3	111.8	113.1	112.8	113.5	113.3	
(b)								
EA	13.7	1.7	8.6	11.3	18.1	5.0	6.2	7.9 ^b
ΔH_f	-34.9	-36.8	-19.5	-20.7	-29.0	-20.8	-26.8	-25.5 ^b

^aFor geometrical parameters see Table II(a).^bFrom Ref. 52.**Scheme 8. Cyclopropyl radical→Allyl radical**

The ring opening of the cyclopropyl radical has been the subject of a comprehensive study by Olivella *et al.*⁵⁰ who confirmed the earlier semiempirical predictions of Dewar and Kirschner⁵¹ that methylene rotation is nonsynchronous, with one methylene group rotated and the C···C bond essen-

tially fully broken before the other methylene group rotates, giving rise to a symmetry broken C_1 transition state (Table VIII).

We were unable to locate experimental geometries for either of these two radicals; however all theoretical models give similar geometrical predictions. The glaring exception is

TABLE X. Methyl radical+formaldehyde→ethoxyl radical. (a) Selected geometrical parameters. (b) Energies (relative to reactants; kcal/mol).

Param.	MNDO	AM1	3-21G	HF	MP2	BLYP	ACM	Expt.
(a)								
Methyl radical (D_{3h}) ^a								
Formaldehyde (C_{2v})								
r_{C-O}	1.216	1.227	1.221	1.184	1.207	1.218	1.204	1.208
r_{C-H}	1.106	1.111	1.083	1.092	1.104	1.121	1.111	1.116
a_{HCH}	113.0	115.5	114.9	115.7	115.7	114.9	115.3	116.5
Transition state (C_s)								
$r_{C_1-C_2}$	2.003	1.953	2.301	2.140	2.073	2.306	2.275	
r_{C_2-O}	1.248	1.267	1.270	1.240	1.222	1.240	1.225	
$a_{C_1C_2O}$	105.5	99.3	101.3	101.9	102.7	104.4	104.3	
Ethoxyl radical (C_s)								
$r_{C_1-C_2}$	1.542	1.515	1.527	1.520	1.519	1.541	1.524	
r_{C_2-O}	1.359	1.335	1.448	1.386	1.391	1.371	1.364	
$a_{C_1C_2O}$	114.7	113.9	111.9	113.4	114.0	116.4	115.7	
(b)								
EA	21.5	8.2	4.7	11.9	19.8	3.4	4.6	6.8 ^b
ΔH_f	-3.6	-14.4	-27.1	-16.7	-5.1	-11.1	-16.4	-10.8 ^b

^aFor geometrical parameters see Table IX(a).^bFrom Ref. 52.

TABLE XI. $\text{H} + \text{HCCH} \rightarrow \text{H}_2 + \text{CCH}$. (a) Selected geometrical parameters. (b) Energies (relative to reactants; kcal/mol).

Param.	MNDO	AM1	3-21G	HF	MP2	BLYP	ACM	Expt.
(a)								
Acetylene								
$r_{\text{C}-\text{C}}$	1.195	1.195	1.188	1.186	1.218	1.215	1.206	1.203
$r_{\text{C}-\text{H}}$	1.051	1.061	1.051	1.057	1.066	1.073	1.067	1.060
Transition state (linear) ^a								
$r_{\text{H}_1-\text{H}_3}$	0.669		0.831	0.830	0.783		0.754	
$r_{\text{C}_1-\text{H}_1}$	2.050		1.462	1.460	1.660		2.055	
$r_{\text{C}_1-\text{C}_2}$	1.195		1.219	1.212	1.180		1.210	
$r_{\text{C}_2-\text{H}_2}$	1.052		1.053	1.058	1.065		1.068	
Hydrogen ^b								
Ethyne radical								
$r_{\text{C}-\text{C}}$	1.195	1.190	1.224	1.215	1.181	1.220	1.210	
$r_{\text{C}-\text{H}}$	1.052	1.064	1.053	1.058	1.065	1.074	1.068	
(b)								
EA	41.7	30.4	32.4	34.0	51.0	25.7	28.4	22.2 ^c
ΔH_f	40.0	30.4	21.1	22.3	46.0	25.7	27.8	

^aThere is apparently no TS on the PES for AM1 and BLYP.^bFor geometrical parameters see Table VI(a).^cFrom Ref. 54.

the nonmethylene hydrogen in the cyclopropyl radical which is predicted to lie in the plane of the ring with MNDO and AM1 and to be bent out of plane (by about 40°) with the *ab initio* methods. Another minor anomaly occurs for the C_1-C_2 bond length which decreases in the transition state for the semiempirical methods, stays essentially the same for the traditional HF-based methods and decreases substantially with the DFT wave functions.

All the theoretical methods give reasonable energetics with ACM showing excellent agreement for both the barrier height and heat of reaction. The MP2 barrier is too high. The semiempirical energetics are also excellent, with MNDO being the best of all.

Scheme 9. Methyl radical + Ethylene → Propyl radical

The addition reaction of the methyl radical to both ethylene and formaldehyde (Scheme 10) has been studied by Gonzalez *et al.*⁵² at various levels of Möller–Plesset perturbation theory. The emphasis in their study was on spin contamination in the UHF wave function and how it affected the barrier height, the principal conclusion being that spin contamination in the transition state artificially raised the barrier for both these reactions and its removal—by spin projection—lowered the calculated barriers by several kcal/mol giving much better agreement with experiment (Table IX).

In line with the above comments, our calculated MP2 barrier for this reaction is much too high. DFT wave functions show very little spin contamination—at least for stable molecules (minima)—and problems from this source are expected to be much less than with UHF wavefunctions. Both the DFT barriers are considerably less than the MP2 one and are in very good agreement with the experimental value quoted by Gonzalez.⁵² All the *ab initio* heats of reaction are

reasonable; the semiempirical values are 10 kcal/mol too low. Overall the ACM energetics are excellent and are clearly the best.

We were unable to find an experimental geometry for the propyl radical, but this species follows the usual trends with BLYP bond lengths longer than the corresponding MP2 values and ACM shorter than BLYP and similar to MP2. The C–C distances are actually shorter for MP2 than for HF, a reversal of the normal situation. All the theoretical methods

TABLE XII. $\langle S^2 \rangle$ of reactants, transition states and products for the six doublet reactions with the HF, MP2, BLYP, and ACM wave functions.

	HF	MP2 ^a	BLYP	ACM
$\text{FO} + \text{H}_2$	0.7621	0.7661	0.7516	0.7525
TS	0.8062	0.8115	0.7533	0.7588
$\text{FOH} + \text{H}$	0.7500	0.7500	0.7500	0.7500
$\text{HO} + \text{H}_2$	0.7551	0.7554	0.7517	0.7520
TS	0.7992	0.7873	0.7544	0.7585
$\text{H}_2\text{O} + \text{H}$	0.7500	0.7500	0.7500	0.7500
Cyclopropyl	0.7601	0.7602	0.7525	0.7536
TS	1.1387	1.1338	0.7790	0.8173
Allyl	0.9727	0.9602	0.7659	0.7874
$\text{CH}_3 + \text{C}_2\text{H}_4$	0.7615	0.7618	0.7533	0.7544
TS	1.0285	0.9900	0.7641	0.7823
$\text{CH}_3\text{CH}_2\text{CH}_2$	0.7623	0.7626	0.7532	0.7577
$\text{CH}_3 + \text{H}_2\text{CO}$	0.7615	0.7618	0.7533	0.7544
TS	0.9429	0.9111	0.7575	0.7669
$\text{CH}_3\text{CH}_2\text{O}$	0.7575	0.7578	0.7522	0.7531
$\text{H} + \text{HCCH}$	0.7500	0.7500	0.7500	0.7500
TS	1.1444	1.0663		0.7860
$\text{H}_2 + \text{CCH}$	1.1873	1.0681	0.7672	0.7878

^a $\langle S^2 \rangle$ for the underlying UHF wave function.

give a similar description of the transition state.

Scheme 10. Methyl radical+formaldehyde→Ethoxyl radical

A related reaction to the above (Scheme 9). Again the calculated MP2 barrier is too high and again the DFT barriers are much lower and in far better agreement with experiment. The DFT heats of reaction are better too. The best energetics are provided by BLYP, AM1, and ACM, in that order (Table X).

We were unable to find an experimental geometry for the ethoxyl radical, but ACM gives the best geometrical parameters for formaldehyde. As was the case with the ethylene reaction, all methods provide a similar description of the transition state, although the forming C···C bond is slightly shorter at the semiempirical level.

Scheme 11. H+HCCH→H₂+CCH

The abstraction of hydrogen from acetylene by a hydrogen atom is an elementary step in the thermolysis of many hydrocarbons. It has been the subject of a number of experimental studies, e.g., Ref. 53, and has been investigated theoretically very recently by Fang and Fu.⁵⁴

We were unable to find an experimental geometry for the ethynyl radical but the experimental bond lengths in acetylene are again well reproduced by ACM. The C–C bond length increases between acetylene and the ethynyl radical with all the *ab initio* methods except MP2, where it shortens significantly. This is yet another manifestation of the effects of spin contamination.⁵⁵

The reaction as written is endothermic and all theoretical methods predict a significant barrier; however the *reverse* reaction, i.e., the reaction of H₂ with CCH, has a very small barrier, and so the heat of reaction and the barrier height for the *forward* reaction are almost identical. Indeed, for AM1 and BLYP the reverse reaction has no barrier and we were unable to locate a transition state with these two methods. The length of the dissociating C···H bond with those methods for which we were able to locate a transition state varies from 1.46 Å at the HF level to in excess of 2 Å with MNDO and ACM (Table XI).

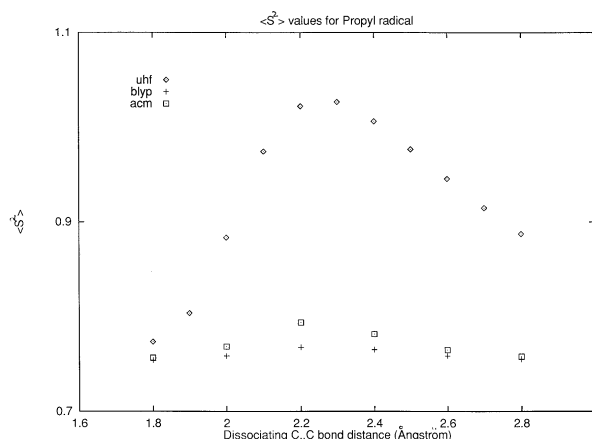


FIG. 2. Plot of $\langle S^2 \rangle$ vs breaking C···C bond distance for dissociation of the propyl radical (Scheme 9) with the UHF, BLYP, and ACM wave functions.

The barrier height is well predicted by both ACM and BLYP. The MP2 barrier is way too high due to the excessive spin contamination in the transition state relative to the reactants (see Table XII); the MP2 reaction energy is probably too endothermic for a similar reason, although this cannot be confirmed as we were unable to find an experimental heat of reaction.

IV. SPIN CONTAMINATION

Before summarizing our results we append some comments on spin contamination which has been mentioned several times when discussing the six radical reactions. All the *ab initio* methods we have used in this work are based on an unrestricted formalism for open shell systems and the presence of spin contamination in this approach can have a major effect on both geometries and energetics. The effects are often particularly marked when the UHF wave function is used as the basis for perturbation expansion, as in the MP2 calculations reported here. The perturbation series converges much more slowly for contaminated species than for relatively spin-pure ones⁵⁶ which means that, when taking energy differences between, say, reactants and products or (especially) reactants and transition states, if one species is more contaminated than the other then its energy will be

TABLE XIII. Average and maximum deviations from experiment for (a) barrier heights (kcal/mol; 12 reactions), (b) heats of reaction (kcal/mol; 10 reactions), and (c) bond lengths (Å; 35 bonds) for all theoretical methods studied.

	MNDO	AM1	3-21G	HF	MP2	BLYP	ACM
(a)							
Av. Error	23.4	9.3	10.4	13.6	9.9	5.9	3.7
Max. Error	51.8	34.2	37.5	30.6	28.8	21.9	12.9
(b)							
Av. Error	10.9	7.5	15.1	10.5	6.3	5.9	6.8
Max. Error	57.7	22.1	36.7	24.8	26.0	13.0	17.7
(c)							
Av. Error	0.020	0.020	0.014	0.014	0.010	0.015	0.008
Max. Error	0.165	0.091	0.041	0.065	0.041	0.034	0.022

(relatively) raised because of this slow convergence and hence the energy difference will be affected. Since transition states, with their often unusual bonding characteristics, are typically more contaminated than minima, spin contamination acts so as to artificially *raise* barrier heights.

Although based on the unrestricted formalism, DFT wave functions show little, if any, spin contamination for stable, open shell molecules.^{57,58} Studies have demonstrated that under the right circumstances DFT wave functions can exhibit minimal contamination over an entire energy surface, including dissociation.⁵⁷ The circumstances are, in fact, right for this to occur for virtually all of the radical reactions considered in this article since in all cases essentially only one species carries all the spin density (see Ref. 57 for more details).

Table XII shows $\langle S^2 \rangle$ values for reactants, transition states and products for all six radical reactions for the HF, MP2, BLYP, and ACM wave functions. All six are doublet reactions for which $\langle S^2 \rangle$ should be 0.75. At the HF and MP2 levels all of the transition states show spin contamination to a greater or lesser degree; relatively minor for OH+H₂, somewhat worse for FO+H₂, and substantial for the other reactions. Two of the products—the allyl and ethynyl radicals—are also highly contaminated. For the DFT wave functions on the other hand, virtually all species are more or less spin pure. For BLYP, $\langle S^2 \rangle$ never rises above 0.78; ACM, which includes a portion of the true exchange, the factor responsible for spin contamination in a UHF wave function,⁵⁷ shows somewhat more contamination, but again it is less than 0.79 in all cases except the transition state for the cyclopropyl ring opening for which it reaches 0.817. For these radical reactions the barrier height at the MP2 level is higher in all cases than for BLYP and ACM and undoubtedly the spin contamination in the underlying UHF wave function plays a major role.

Figure 2 presents a schematic plot of $\langle S^2 \rangle$ vs breaking C...C bond distance for the dissociation of the propyl radical (Scheme 9) with the UHF, BLYP, and ACM wave functions. Starting from the propyl radical, as the dissociating C...C bond distance increases, spin contamination builds up rapidly for UHF, reaches a maximum in the TS region, and declines slowly thereafter as dissociation becomes complete; note that contamination is significant even at quite large C...C distances. For ACM and BLYP, the situation is similar but on a dramatically reduced scale; the maximum is reached in the TS region as with UHF, but this maximum is basically a “blip” and the entire dissociation can in both cases be considered as essentially spin pure. (See *Note added in proof*.)

V. CONCLUSIONS

What are we to conclude from this, albeit limited, study? Although we have only looked at twelve reactions, we consider that we are justified in drawing the following conclusions (bearing in mind the limitations of our basis set).

(1) Barrier heights calculated with BLYP are almost always *lower* than barriers calculated with MP2, particularly for radical reactions. In the latter case, spin contamination in

the underlying UHF wave function plays a large part in artificially raising the MP2 barrier.

(2) BLYP barriers for radical reactions tend to be *too* low compared to experiment. In particular, reactions with very low barriers may be erroneously predicted to have no barrier at all (e.g., OH+H₂ and CCH+H₂, this work).

(3) ACM barriers tend to be *higher* than the corresponding BLYP barrier, particularly for radical reactions, and are typically in better agreement with experiment. For radicals, ACM barriers are still lower than with MP2.

(4) Although giving at least as good energetics on the average as MP2, there are some disturbing instances (OH+H₂) where the BLYP PES shows “unusual” behavior suggesting that all is not well with this particular functional. (The unusual behavior on this energy surface is not confined to the BLYP functional; see Ref. 49.) The ACM functional, which includes a portion of the exact Hartree–Fock exchange, appears to rectify the situation and restore “normal” behavior.

(5) The ACM method gives excellent geometries which are often in better agreement with experiment than MP2. BLYP geometries, on the other hand, are poor with bond lengths that are typically much too long.

Table XIII gives average and maximum deviations from experiment for barrier heights, heats of reaction, and bond lengths for all the theoretical methods studied. Examination of these results clearly shows the ACM functional to be the best. It appears to be significantly better than MP2, especially for barrier heights. This conclusion is also confirmed by the much larger study of reaction energies and geometries we have undertaken mentioned in Sec. I.¹⁴ All the correlated methods are, not surprisingly, better than Hartree–Fock, and—given its relative cheapness in terms of CPU time—so is AM1, which for reaction energetics provides results of only slightly worse quality than MP2 at a fraction of the cost.

Overall, our results—along with many others in the literature—are very encouraging for density functional methods. However, there *are* problems with the current crop of density functionals and further developments on the functionals themselves are likely in the near future. Whether these difficulties can be resolved without the aid of the exact exchange remains to be seen.

Note added in proof. Pople *et al.* have recently argued⁵⁹ that Kohn–Sham (KS) calculations on open shell systems should naturally be spin unrestricted in character and hence will be spin contaminated to a certain degree. The “correct” amount of spin contamination is unknown, although current functionals exhibit only minor contamination, in agreement with the observations made in this work and elsewhere. We thank Dr. N. C. Handy for sending us a preprint of Ref. 59.

ACKNOWLEDGMENT

This work was supported in part by a grant to Biosym Technologies from the National Institute of Standards and Technology/Advanced Technology Program.

APPENDIX

Total energies of all species examined at all levels of theory and HF/6-31G* zero point vibrational energies. *Ab initio* values are total energies in hartree; semiempirical val-

ues are heats of formation (originally in kcal/mol but converted into hartree). Relative *ab initio* energies (kcal/mol) reported in Tables I–XI have been corrected using the quoted ZPVE's scaled by 0.89.

	MNDO	AM1	3-21G	HF	MP2	BLYP	ACM	ZPVE
Vinyl Alcohol								
	-0.05567	-0.05351	-152.04177	-152.88783	-153.32113	-153.74545	-153.75015	0.06105
Vinyl Alcohol <---> Acetaldehyde TS								
	0.08971	0.06387	-151.91310	-152.77010	-153.22673	-153.66177	-153.66071	0.05423
Acetaldehyde								
	-0.06746	-0.06631	-152.05525	-152.91517	-153.34799	-153.77009	-153.77389	0.05993
trans-Butadiene								
	0.04603	0.04757	-154.05946	-154.91904	-155.42688	-155.89978	-155.93369	0.09153
Ethylene								
	0.02449	0.02620	-77.60099	-78.03136	-78.28701	-78.53488	-78.55763	0.05774
trans-Butadiene + Ethylene <---> Cyclohexene TS								
	0.14977	0.11163	-231.60321	-232.87893	-233.68572	-234.40200	-234.46026	0.15066
Cyclohexene								
	-0.01600	-0.01612	-231.72915	-233.01869	-233.79830	-234.49212	-234.57216	0.15705
Tetrazine								
	0.10941	0.15519	-292.88939	-294.59158	-295.48511	-296.24807	-296.21003	0.05668
Tetrazine <---> Hydrogen Cyanide + Nitrogen TS								
	0.26480	0.27085	-292.81026	-294.47005	-295.41257	-296.19240	-296.12584	0.04770
Hydrogen Cyanide								
	0.05667	0.04937	-92.35408	-92.87454	-93.16694	-93.39615	-93.38234	0.01798
Nitrogen								
	0.01397	0.01775	-108.30095	-108.94319	-109.25389	-109.50614	-109.47832	0.00629
Trifluoromethanol								
	-0.34283	-0.36181	-409.41794	-411.64413	-412.45687	-413.40147	-413.31917	0.03197
Trifluoromethanol <---> Carbonyl Fluoride + Hydrogen Fluoride TS								
	-0.19741	-0.25657	-409.32013	-411.54383	-412.38133	-413.34172	-413.24825	0.02573
Carbonyl Fluoride								
	-0.22093	-0.23317	-309.90428	-311.61246	-312.25134	-312.97361	-312.90018	0.01579
Hydrogen Fluoride								
	-0.09521	-0.11838	-99.46022	-100.00078	-100.18088	-100.40240	-100.38812	0.00987

	MNDO	AM1	3-21G	HF	MP2	BLYP	ACM	ZPVE
Cyclobutene								
	0.04932	0.07282	-154.03072	-154.89898	-155.41451	-155.87742	-155.92214	0.09322
Cyclobutene <---> trans-Butadiene TS								
	0.12866	0.12913	-153.96435	-154.82434	-155.35475	-155.82736	-155.86207	0.09033
trans-Butadiene see above								
trans-Butadiene <---> cisoid-Butadiene TS								
	0.04676	0.05070	-154.05046	-154.90937	-155.41737	-155.88687	-155.92196	0.09086
Cisoid-Butadiene								
	0.04648	0.04879	-154.05514	-154.91420	-155.42265	-155.89375	-155.92811	0.09149
Fluorine Oxide radical								
	0.03246	0.03443		-174.11990	-174.43597	-174.86121	-174.80639	0.00265
Hydrogen								
	0.00115	-0.00826	-1.12296	-1.12683	-1.14414	-1.16526	-1.17473	0.01058
Fluorine Oxide + Hydrogen <---> Hydrogen Fluoroxide + H atom TS								
	0.09934	0.05962		-175.18801	-175.54373	-176.00184	-175.95395	0.01181
Hydrogen Fluoroxide								
	-0.02972	-0.03603	-173.80067	-174.72664	-175.08625	-175.50607	-175.46045	0.01554
H atom								
	0.08303	0.08303	-0.49620	-0.49823	-0.49823	-0.49545	-0.50213	0.00000
Hydroxyl radical								
	0.00035	0.00101	-74.97023	-75.38106	-75.51990	-75.70518	-75.69518	0.00906
Hydrogen see above								
Hydroxyl + Hydrogen <---> Water + H atom TS								
	0.05042	0.01100	-76.05243	-76.46549	-76.64358	-76.87158	-76.86447	0.01946
Water								
	-0.09714	-0.09443	-75.58596	-76.00934	-76.19557	-76.38627	-76.38259	0.02291
H atom see above								
Cyclopropyl radical								
	0.08055	0.09421	-115.75662	-116.41509	-116.78126	-117.13727	-117.17725	0.07228
Cyclopropyl <---> Allyl TS								
	0.11736	0.13333	-115.72100	-116.37226	-116.72036	-117.10410	-117.13348	0.06737
Allyl radical								
	0.04036	0.04804	-115.82304	-116.46764	-116.81340	-117.18672	-117.21747	0.06950

	MNDO	AM1	3-21G	HF	MP2	BLYP	ACM	ZPVE
Methyl radical								
	0.03921	0.04771	-39.34261	-39.55875	-39.67303	-39.80434	-39.82451	0.03096
Ethylene see above								
Methyl + Ethylene <---> Propyl TS								
	0.08556	0.07661	-116.93288	-117.57520	-117.93431	-118.33438	-118.37525	0.08915
Propyl radical								
	0.00806	0.01530	-116.98249	-117.63083	-118.01402	-118.38019	-118.43252	0.09443
Formaldehyde								
	-0.05245	-0.05023	-113.22182	-113.86569	-114.16773	-114.46920	-114.45635	0.02920
Methyl radical see above								
Formaldehyde + Methyl <---> Ethoxyl TS								
	0.02100	0.01051	-152.56182	-153.41031	-153.81411	-154.27311	-154.27847	0.06569
Ethoxyl radical								
	-0.01894	-0.02544	-152.61640	-153.45984	-153.85772	-154.29995	-154.31575	0.07001
Acetylene								
	0.09220	0.08729	-76.39596	-76.81732	-77.06860	-77.28882	-77.29252	0.02940
H atom see above								
Acetylene + H atom <---> Ethynyl + Hydrogen TS								
	0.24173	0.21872	-76.83705	-77.25780	-77.48222	-77.73991	-77.74594	0.02545
Ethynyl radical								
	0.23782	0.22696	-75.73206	-76.14979	-76.34605	-76.57467	-76.57223	0.01498
Hydrogen see above								

¹P. Hohenberg and W. Kohn, Phys. Rev. B **136**, 864 (1964); W. Kohn and L. J. Sham, Phys. Rev. A **140**, 1133 (1965).

²T. Ziegler, Chem. Rev. **91**, 651 (1991), and references therein.

³*Density Functional Methods in Chemistry*, edited by J. Labanowski and J. Andzelm (Springer-Verlag, New York, 1991).

⁴J. Andzelm and E. Wimmer, J. Chem. Phys. **96**, 1280 (1992).

⁵B. G. Johnson, P. M. W. Gill, and J. A. Pople, J. Chem. Phys. **98**, 5612 (1993).

⁶B. Delley, J. Chem. Phys. **92**, 508 (1990).

⁷A. D. Becke, Phys. Rev. A **38**, 3098 (1988).

⁸C. Lee, W. Yang, and R. G. Parr, Phys. Rev. B **37**, 785 (1988).

⁹J. P. Perdew, in *Electronic Structure of Solids*, edited by P. Ziesche and H. Eschrig (Akademie Verlag, Berlin, 1991).

¹⁰C. W. Murray, N. C. Handy, and R. D. Amos, J. Chem. Phys. **98**, 7145 (1993).

¹¹G. Fitzgerald and J. Andzelm, J. Phys. Chem. **95**, 10 531 (1991).

¹²N. Godbout, D. R. Salahub, J. Andzelm, and E. Wimmer, Can. J. Chem. **70**, 560 (1992).

¹³G. J. Laming, V. Termath, and N. C. Handy, J. Chem. Phys. **99**, 8765 (1993).

¹⁴A. C. Scheiner, J. Baker, and J. Andzelm (unpublished).

¹⁵L. A. Curtiss, K. Raghavachari, G. W. Trucks, and J. A. Pople, J. Chem. Phys. **94**, 7221 (1991).

¹⁶L. Fan and T. Ziegler, J. Chem. Phys. **92**, 3645 (1990).

¹⁷J. Andzelm, C. Sosa, and R. A. Eades, J. Phys. Chem. **97**, 4664 (1993).

¹⁸R. V. Stanton and K. M. Merz, J. Phys. Chem. **100**, 434 (1994).

¹⁹C. A. Gonzalez and B. G. Johnson, Poster at satellite symposium of 8th International Congress of Quantum Chemistry, Cracow, Poland, June 13–16, 1994 (unpublished).

²⁰K. Raghavachari, D. L. Strout, G. K. Odom, G. E. Scuseria, J. A. Pople, B. G. Johnson, and P. M. W. Gill, Chem. Phys. Lett. **214**, 357 (1993).

²¹J. A. Pople, Conference on Current Trends in Computational Chemistry, Jackson, Mississippi, Nov. 1993 (unpublished).

²²A. D. Becke, J. Chem. Phys. **98**, 5648 (1993).

²³M. J. Frisch, M. Head-Gordon, G. W. Trucks, J. B. Foresman, H. B. Schlegel, K. Raghavachari, M. A. Robb, J. S. Binkley, C. Gonzalez, D. J. Defrees, D. J. Fox, R. A. Whiteside, R. Seeger, C. F. Melius, J. Baker, R. L. Martin, L. R. Kahn, J. J. P. Stewart, S. Topiol, and J. A. Pople, GAUSSIAN 90 (Gaussian Inc., Pittsburgh PA, 1990).

²⁴R. Ahlrichs, M. Bär, M. Ehrig, M. Häser, H. Horn, and C. Kölmel, TURBOMOLE, v.2.3, Biosym Technologies, San Diego, CA (1993).

²⁵J. Baker, J. Comp. Chem. **7**, 385 (1986).

²⁶J. Baker, OPTIMIZE, v.1.0 beta, Biosym Technologies, San Diego, CA (1993).

²⁷J. Baker, J. Andzelm, A. Scheiner, and B. Delley, J. Chem. Phys. **101**, 8894 (1994).

²⁸P. M. W. Gill, B. G. Johnson, and J. A. Pople, Chem. Phys. Lett. **209**, 506 (1993).

²⁹B. G. Johnson, P. M. W. Gill, and J. A. Pople, Chem. Phys. Lett. **220**, 377 (1994).

- ³⁰D. R. Lide, Editor, *Handbook of Chemistry and Physics*, 74th Ed. (CRC, Boca Raton, FL, 1993).
- ³¹B. J. Smith, M. T. Nguyen, W. J. Bouma, and L. Radom, *J. Am. Chem. Soc.* **113**, 6452 (1991).
- ³²J. H. Holmes and F. P. Lossing, *J. Am. Chem. Soc.* **104**, 2648 (1982).
- ³³K. Lammertsma and B. V. Prasad, *J. Am. Chem. Soc.* **116**, 642 (1994).
- ³⁴F. Bernardi, A. Bottoni, M. J. Field, M. F. Guest, I. H. Hillier, M. A. Robb, and A. Venturini, *J. Am. Chem. Soc.* **110**, 3050 (1988), and references therein.
- ³⁵M. J. S. Dewar, S. Olivella, and J. J. P. Stewart, *J. Am. Chem. Soc.* **108**, 5771 (1986).
- ³⁶K. N. Houk, R. J. Loncharich, J. F. Blake, and W. L. Jorgensen, *J. Am. Chem. Soc.* **111**, 9172 (1989).
- ³⁷D. A. Hrovat, K. Morokuma, and W. T. Borden, *J. Am. Chem. Soc.* **116**, 1072 (1994).
- ³⁸A. R. Katritzky, *Handbook of Heterocyclic Chemistry* (Pergamon, New York, 1985).
- ³⁹A. C. Scheiner, G. E. Scuseria, and H. F. Schaefer, *J. Am. Chem. Soc.* **108**, 8160 (1986).
- ⁴⁰S. G. Lias, J. E. Bartmess, J. F. Liebman, J. L. Holmes, R. D. Levin, and W. G. Mallard, *J. Phys. Chem. Ref. Data* **17**, Suppl. 1 (1988).
- ⁴¹J. Overend and J. R. Scherer, *J. Chem. Phys.* **32**, 1296 (1960).
- ⁴²J. S. Francisco, *Chem. Phys. Lett.* **218**, 401 (1994).
- ⁴³D. C. Spellmeyer and K. N. Houk, *J. Am. Chem. Soc.* **110**, 3412 (1988).
- ⁴⁴D. Bond, *J. Org. Chem.* **55**, 661 (1990).
- ⁴⁵K. B. Wiberg, R. E. Rosenberg, and P. R. Rablen, *J. Am. Chem. Soc.* **113**, 2890 (1991).
- ⁴⁶J. E. Rice, B. Liu, T. J. Lee, and C. M. Rohlfing, *Chem. Phys. Lett.* **161**, 277 (1989).
- ⁴⁷I. L. Alberts and H. F. Schaefer, *Chem. Phys. Lett.* **161**, 375 (1989).
- ⁴⁸J. S. Francisco, *J. Chem. Phys.* **100**, 2896 (1994).
- ⁴⁹J. Baker, J. Andzelm, and M. Muir (unpublished).
- ⁵⁰S. Olivella, A. Sole, and J. M. Bofill, *J. Am. Chem. Soc.* **112**, 2160 (1990).
- ⁵¹M. S. J. Dewar and S. J. Kirschner, *J. Am. Chem. Soc.* **96**, 5244 (1974).
- ⁵²C. Gonzalez, C. Sosa, and H. B. Schlegel, *J. Phys. Chem.* **93**, 2435 (1989).
- ⁵³P. Dagaut, M. Cathonnet, and J. C. Boettner, *Int. J. Chem. Kinet.* **23**, 437 (1991).
- ⁵⁴D. C. Fang and X. Y. Fu, *Int. J. Quant. Chem.* **49**, 3 (1994).
- ⁵⁵J. Baker, *J. Chem. Phys.* **91**, 1789 (1989).
- ⁵⁶N. C. Handy, P. J. Knowles, and K. Somasundram, *Theor. Chim. Acta* **68**, 87 (1985).
- ⁵⁷J. Baker, A. Scheiner, and J. Andzelm, *Chem. Phys. Lett.* **216**, 380 (1993).
- ⁵⁸G. J. Laming, N. C. Handy, and R. D. Amos, *Mol. Phys.* **80**, 1121 (1993).
- ⁵⁹J. A. Pople, P. M. W. Gill, and N. C. Handy, *Int. J. Quant. Chem.* (to be published).